

Measurements of plasma temperature and electron density in laser-induced copper plasma by time-resolved spectroscopy of neutral atom and ion emissions

V K UNNIKRISHNAN¹, KAMLESH ALTI¹, V B KARTHA¹, C SANTHOSH^{1,*},
G P GUPTA² and B M SURI²

¹Centre for Atomic and Molecular Physics, Manipal University, Manipal 576 104, India

²Laser and Plasma Technology Division, Bhabha Atomic Research Centre,
Mumbai 400 085, India

*Corresponding author. E-mail: santhosh.cls@manipal.edu

MS received 7 January 2010; revised 3 February 2010; accepted 4 February 2010

Abstract. Plasma produced by a 355 nm pulsed Nd:YAG laser with a pulse duration of 6 ns focussed onto a copper solid sample in air at atmospheric pressure is studied spectroscopically. The temperature and electron density characterizing the plasma are measured by time-resolved spectroscopy of neutral atom and ion line emissions in the time window of 300–2000 ns. An echelle spectrograph coupled with a gated intensified charge coupled detector is used to record the plasma emissions. The temperature is obtained using the Boltzmann plot method and the electron density is determined using the Saha–Boltzmann equation method. Both parameters are studied as a function of delay time with respect to the onset of the laser pulse. The results are discussed. The time window where the plasma is optically thin and is also in local thermodynamic equilibrium (LTE), necessary for the laser-induced breakdown spectroscopy (LIBS) analysis of samples, is deduced from the temporal evolution of the intensity ratio of two Cu I lines. It is found to be 700–1000 ns.

Keywords. Laser-induced plasma; spectroscopy; plasma temperature; electron density.

PACS Nos 52.50.Jm; 52.70.Kz; 52.25.Os

1. Introduction

Pulsed laser-induced plasmas (LIPs) of metals and alloys formed at laser pulse irradiances near the plasma ignition threshold are of great interest since they have several important applications, e.g. material processing, thin film deposition and metal analysis in solid samples [1]. Optical emission spectra of an LIP consist of atomic and ionic lines, superimposed on a continuum of radiation. Elemental analysis of the sample based on the optical emission spectra from an LIP is known as

laser-induced plasma spectroscopy (LIPS), also called as laser-induced breakdown spectroscopy (LIBS). The LIBS technique, utilizing a pulsed LIP formed near the plasma ignition threshold as a spectroscopic source is a well-known analytical technique to provide remote, *in-situ*, rapid and multi-elemental analysis of bulk and trace sample in any phase (solid, liquid and gas) with no or minimal sample preparation [2–4].

The characterization of LIPs by determining their temperature and electron density is essential and has gained considerable interest in recent years for the understanding and exploitation of these complex and versatile spectroscopic sources. The plasma characteristics are dependent on laser irradiance, wavelength, pulse duration, target material, atmospheric conditions, space and time. For elemental analysis using LIBS, it is important that LIP should be optically thin and in LTE

Under LTE condition in the plasma, the excitation temperature governing the distribution of energy level excitation through the Boltzmann equation and the ionization temperature governing the ionization equilibrium through the Saha equation are equal to the electronic temperature describing the Maxwellian distribution of electron velocities [5]. Thus, one describes the plasma in LTE by a common temperature T , called the plasma temperature. Optical emission spectroscopy has recently attracted a lot of attention for characterizing an LIP. The most widely used spectroscopic method for the determination of T is the Boltzmann plot method [5] which employs the ratio of integrated line intensities for two or more atomic lines. Among several diagnostic methods for measuring the plasma electron density n_e , plasma spectroscopy based on either Stark broadening of spectral lines or the Saha–Boltzmann equation is considered as the simplest method [5].

For the spectroscopic investigation of solid targets, several workers studied LIP from solid copper. Lee *et al* [6] carried out time-integrated, space-resolved studies of laser-ablated plasma emission with Cu target in air at atmospheric pressure using a 193 nm pulsed excimer laser and determined T using the emission spectra. Mao *et al* [7] characterized an LIP from a solid Cu target in air using a 248 nm pulsed excimer laser. They have employed time-integrated emission spectroscopy in the plasma characterization. Pietch and his co-workers [8] studied the expansion of Cu plasma and its distribution, formed by a 308 nm pulsed excimer laser in air at reduced pressure (20 mTorr), using a gated intensified charge-coupled device (ICCD) camera for spectroscopic applications. Wu *et al* [9] investigated the dynamics of Cu plasma generated by a 308 nm pulsed excimer laser in air at reduced pressure (<1 mTorr) by optically examining the plasma plume. Hafez *et al* [10] studied the characteristics of Cu plasma produced by a 355 nm pulsed Nd:YAG laser interaction with a solid target in vacuum and argon buffer gas using the plasma spectroscopy and Langmuir probe methods. They determined T using the Boltzmann plot and n_e using the Stark line broadening.

In this paper, we report the measurements of plasma temperature T and electron density n_e in Cu plasma formed by irradiation of a solid Cu target in air at atmospheric pressure with a 355 nm pulsed Nd:YAG laser, using time-resolved spectroscopy of atom and ion emissions with a gated ICCD camera coupled with an echelle spectrograph. The laser irradiance of 4.5×10^8 W/cm² employed in this work was near the plasma ignition threshold. The aim of this investigation was to identify and optimize laser ablation parameters suitable for elemental composition

analysis of samples using the LIBS technique. We have used the Boltzmann plot method for determining T and the Saha–Boltzmann equation method for determining n_e , instead of using Stark line broadening. From these measurements we have found the time window where the plasma is optically thin and in LTE, which is a necessary requirement for the applicability of the equilibrium equations and emission signals to elemental analysis using the LIBS technique.

2. Experimental details

The schematic diagram of the experimental set-up for the LIBS study is presented in figure 1. The Q-switched Nd:YAG laser (Spectra Physics PRO 230-10) was operated at the third harmonic wavelength of 355 nm, pulse width of 6 ns and repetition rate of 10 Hz. The laser was focussed on a solid copper target placed in air at atmospheric pressure using a bi-convex lens of focal length 20 cm. This provides a laser pulse irradiance of 4.5×10^8 W/cm², which is near to the plasma ignition threshold, forming the plasma over the target surface. The target was placed on an X–Y translation stage having a speed of 6 mm/s so that every laser pulse was incident on a fresh location of the target. The spatially integrated plasma light emission was collected and imaged onto the spectrograph slit using an optical fibre-based collection system. This collection system was positioned at a distance of about 20 cm from the plasma, making an angle 45° to the laser beam. An echelle spectrograph–ICCD system (Andor Mechelle ME5000-DH734-18U-03PS150) was used to record the emission spectrum. The spectrograph with an echelle grating covers 200–975 nm spectral range in one setting with a good wavelength resolution (0.05 nm). The spectrally dispersed light from the spectrograph was collected by a thermoelectrically cooled ICCD camera which is sensitive in the whole UV–VIS–NIR region, converting the spectral signal into digital signal. The detector was

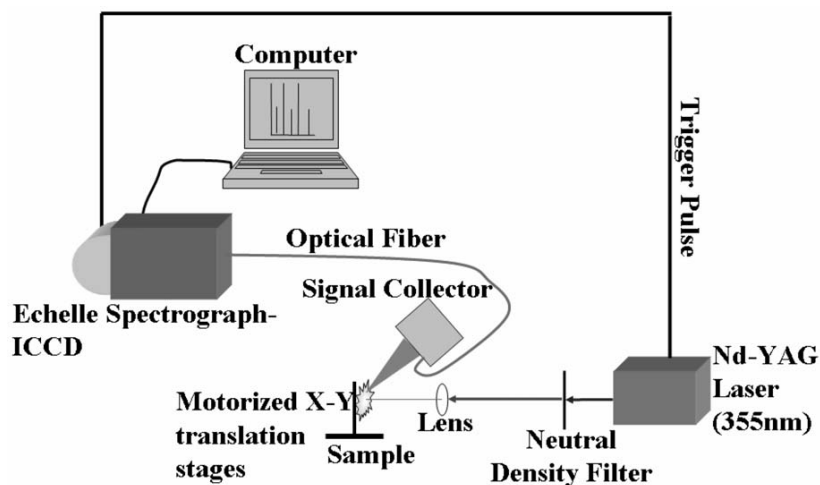


Figure 1. Experimental lay-out of LIBS system.

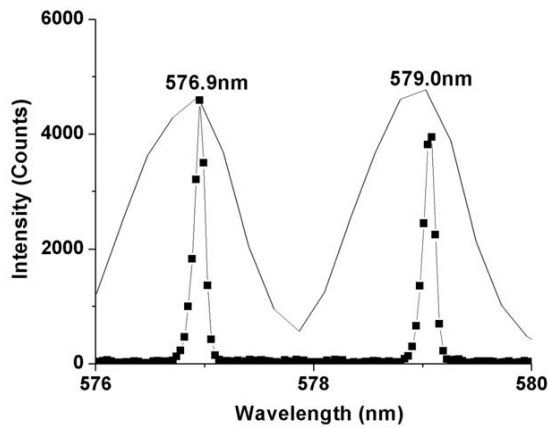


Figure 2. Mercury doublet spectrum recorded using echelle spectrograph (dotted lines) and Czerny-turner spectrograph (continuous lines).

gated in synchronization with the laser pulse to get maximum signal-to-noise ratio. The detector gate width was kept constant at 750 ns whereas its delay time was varied in the time span 300–2000 ns for recording the plasma emission signals. A Hg–Ar lamp, which provides sharp lines from 200 to 1000 nm, was used for wavelength calibration of this system. Intensity calibration of the echelle spectrograph–ICCD system was done using NIST certified deuterium–quartz–tungsten–halogen lamp (Ocean Optics, USA).

The unique feature of the LIBS system used for our study is the usage of an echelle spectrograph which provides broad spectral coverage with a good resolution. The echelle spectrograph disperses the spectral components of the collected plasma light in both X and Y directions to fill a 2D CCD. Echelle spectrographs differ from Czerny-turner spectrographs in the fact that the first one has got two dispersive elements (a dual order prism and a grating) whereas the latter has only one grating. These elements disperse light at 90° to one another. Hence the spread-out light on the CCD gives both X and Y spectral information. This provides wide spectral band pass, as given by a low-dispersion Czerny-turner, together with highest resolution of a high-dispersion Czerny-turner. It is observed that the resolution of the spectrum recorded with the echelle spectrograph is better by a factor of ~ 10 compared to Czerny-turner spectrograph as shown in figure 2. Apart from this, in the present echelle spectrograph there are no moving parts which make the system more convenient and reliable for calibration and fast analysis. This echelle spectrograph–ICCD system will be useful for multi-elemental composition analysis of samples using the LIBS technique planned in future.

3. Theoretical description

For the interpretation of spectroscopic data, one requires a plasma ionization model to describe the ionization state and atom/ion energy level populations in terms

of plasma temperature and electron density. We present below the methods for determining the LIP parameters T and n_e for optically thin and LTE plasmas.

3.1 Boltzmann plot method for T

For plasma in LTE, the energy level populations of the species are given by the Boltzmann distribution law [5],

$$\frac{n_{k,Z}}{n_Z} = \frac{g_{k,Z}}{P_Z} \exp\left(-\frac{E_{k,Z}}{k_B T}\right). \quad (1)$$

Here, the index Z refers to the ionization stage of the species ($Z = 0$ and 1 corresponding to the neutral and singly ionized atoms respectively), k_B is the Boltzmann constant, T is the plasma temperature, $n_{k,Z}$, $E_{k,Z}$ and $g_{k,Z}$ are the population, energy and degeneracy of the upper energy level k respectively, n_Z is the number density and P_Z is the partition function of the species in ionization stage Z . The integrated intensity I_Z of a spectral line occurring between the upper energy level k and the lower energy level i of the species in ionization stage Z in optically thin plasma, i.e. plasma in which only very little radiation is absorbed, is given as

$$I_Z = \frac{hc}{4\pi\lambda_{ki,Z}} A_{ki,Z} n_{k,Z} L, \quad (2)$$

where h is the Planck constant, c is the speed of light, L is the characteristic length of the plasma, $A_{ki,Z}$ is the transition probability and $\lambda_{ki,Z}$ is the transition line wavelength. Using eq. (1), eq. (2) can be rewritten as

$$I_Z = \frac{hc}{4\pi\lambda_{ki,Z}} A_{ki,Z} L \frac{n_Z}{P_Z} g_{k,Z} \exp\left(-\frac{E_{k,Z}}{k_B T}\right). \quad (3)$$

By taking the natural logarithm, eq. (3) can be rewritten as

$$\ln\left(\frac{I_Z \lambda_{ki,Z}}{g_{k,Z} A_{ki,Z}}\right) = -\frac{1}{k_B T} E_{k,Z} + \ln\left(\frac{hcLn_Z}{4\pi P_Z}\right). \quad (4)$$

This yields a linear plot (the so-called Boltzmann plot) if one represents the magnitude on the left-hand side for several transitions against the energy of the upper level of the species in ionization stage Z . The value of T is deduced from the slope of the Boltzmann plot. As eq. (4) is obtained under the assumption of plasma being optically thin as well as in LTE, the applicability of this equation is limited to LTE and optically thin plasmas.

3.2 Saha-Boltzmann equation method for n_e

The electron density using atom and ion spectral lines emitted from the plasma is determined from the Saha-Boltzmann equation as [5,11]

$$n_e = \frac{I_Z^*}{I_{Z+1}^*} 6.04 \times 10^{21} (T)^{3/2} \times \exp[(-E_{k,Z+1} + E_{k,Z} - \chi_Z)/k_B T] \text{ cm}^{-3}, \quad (5)$$

where $I_Z^* = I_Z \lambda_{ki,Z} / g_{k,Z} A_{ki,Z}$ and χ_Z is the ionization energy of the species in the ionization stage Z . The lowering of the ionization energy due to the interactions in the plasma is negligibly small which has been omitted in eq. (5).

3.3 Optically thin plasma

The elemental composition analysis from the line intensities in a LIBS experiment becomes simple if the plasma is optically thin and is also in LTE. It is thus necessary to know the time window for time-evolving plasma like LIPs where the plasma is optically thin as well as in LTE. Using eq. (3), the intensity ratio of two lines of the same species of ionization stage Z is expressed as

$$\frac{I_1}{I_2} = \left(\frac{\lambda_{nm,Z}}{\lambda_{ki,Z}} \right) \left(\frac{A_{ki,Z}}{A_{nm,Z}} \right) \left(\frac{g_{k,Z}}{g_{n,Z}} \right) \exp \left(-\frac{E_{k,Z} - E_{n,Z}}{k_B T} \right), \quad (6)$$

where I_1 is the line intensity from the $k-i$ transition and I_2 is that from the $n-m$ transition. If we consider two emission lines having the same upper level or as close

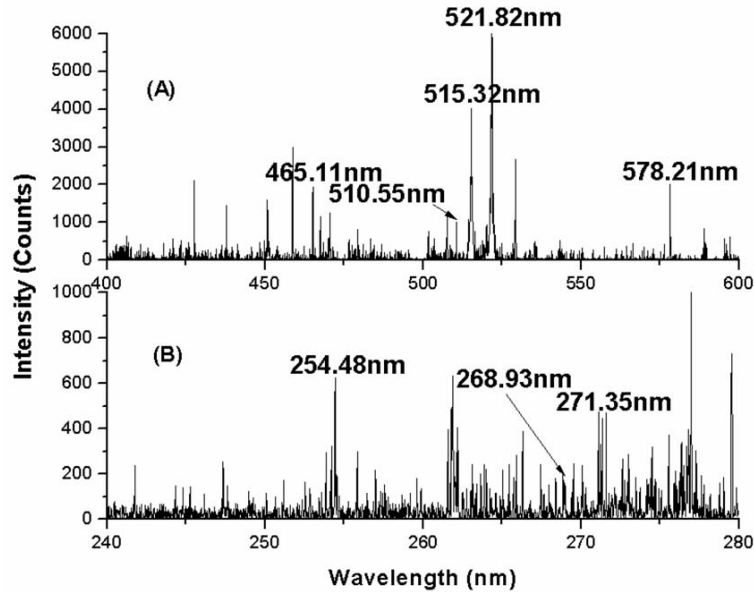


Figure 3. LIBS spectra of copper recorded using ICCD-based echelle spectrograph with a gate delay time of 700 ns at a laser irradiance of $4.5 \times 10^8 \text{ W/cm}^2$, showing (A) Cu I atomic lines and (B) Cu II ionic lines used for the characterization of the laser-induced Cu plasma.

Table 1. Wavelength, lower and upper energy levels, upper level degeneracy and transition probability for the Cu I and Cu II emission lines used in this work.

Atom/ion	Wavelength (nm)	Upper level energy (eV)	Lower level energy (eV)	Upper level degeneracy	Transition probability (s^{-1})
Cu I	465.11	7.740	5.072	8	3.8×10^7
Cu I	510.55	3.817	1.389	4	2.0×10^6
Cu I	515.32	6.191	3.786	4	6.0×10^7
Cu I	521.82	6.192	3.817	6	7.5×10^7
Cu I	578.21	3.786	1.642	2	1.65×10^7
Cu II	268.93	13.392	8.783	7	4.1×10^7
Cu II	271.35	13.432	8.864	5	6.8×10^7

as possible, the temperature effect of the Boltzmann factor on the reproducibility of the line intensity ratio is minimized and at the same time the consideration of the efficiency factor of the collecting system is avoided. Neglecting the exponential factor in that condition, one can find out the theoretical value of the intensity ratio of the two lines by using the atomic parameters of the transitions. By matching this ratio with the measured values at different delay times, one finds out the time window where the plasma is optically thin.

4. Results and discussion

Using the neutral atom and ion emission spectra recorded at different delay times in the time span 300–2000 ns, we have characterized the LIP in terms of its transient T and n_e . Figure 3 shows a typical spectrum recorded using ICCD-based echelle spectrograph with a gate delay time of 700 ns, depicting Cu I and Cu II emission lines from the LIP. Five Cu I and two Cu II emission lines which are well resolved and free from spectral interference are chosen in the present work. These lines along with their spectroscopic parameters, taken from the NIST atomic database [12], are shown in table 1. The value of T is obtained from the Boltzmann plot made from the analysis of the five recorded Cu I lines at a given delay time. Figure 4 shows one such Boltzmann plot from the intensities of these Cu I lines at a delay time of 700 ns, the slope of which gives $T = 0.79$ eV. The estimated values of T at several delay times are presented in table 2. These are plotted in figure 5. It is observed that after 500 ns delay time the plasma cools down exponentially.

The value of n_e is obtained from eq. (5) using the measured intensity ratio of Cu I and Cu II lines at a given delay time. We have considered three intensity ratios, 515.32 nm Cu I and 268.93 nm Cu II, 515.32 nm Cu I and 271.35 nm Cu II and 521.82 nm Cu I and 268.93 nm Cu II and obtained the values of n_e . As seen from figure 3, Cu II lines at 277 and 279 nm are more intense than the chosen Cu II lines for the analysis. However, we could not use these more intense Cu II lines as the Cu II line at 277 nm overlaps with the three Cu I lines at 276.637, 276.639 and 276.888 nm and the transition probability of the Cu II line at 279 nm is not

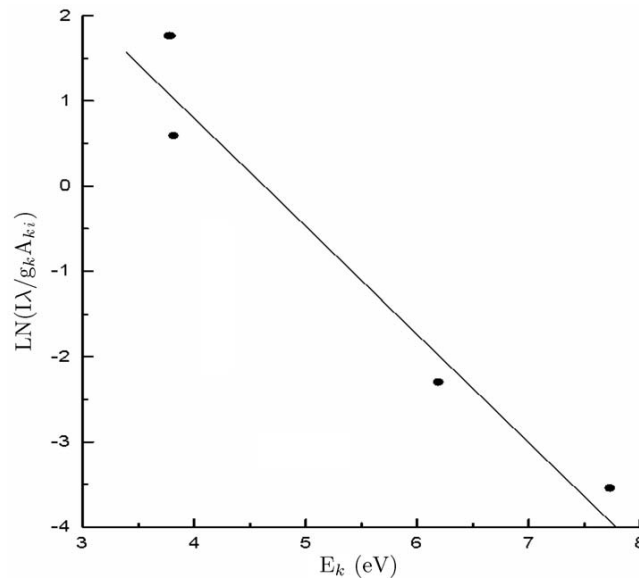


Figure 4. Boltzmann plot made from the analysis of five Cu I lines, 465.11, 510.55, 515.32, 521.82 and 578.21 nm, considering the intensities at a delay time of 700 ns. The continuous line represents the result of a linear best fit. I and λ are the intensity and the wavelength of a transition from upper level k of energy E_k and statistical weight g_k to lower level i with A_{ki} as the corresponding transition probability. The slope gives the temperature as 0.79 eV.

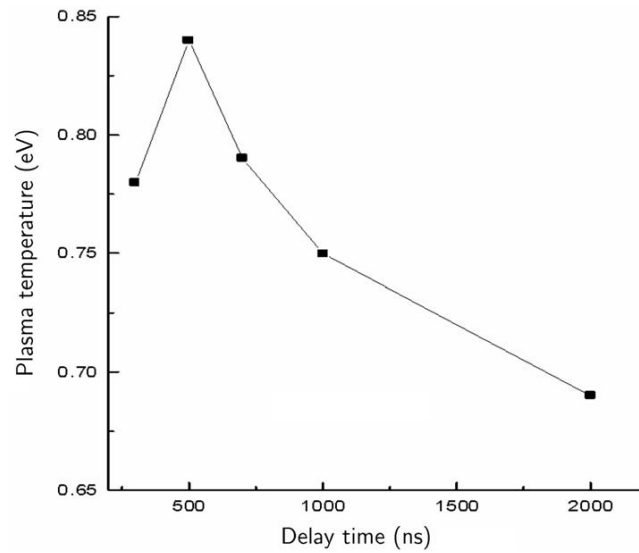


Figure 5. Variation of plasma temperature with delay time.

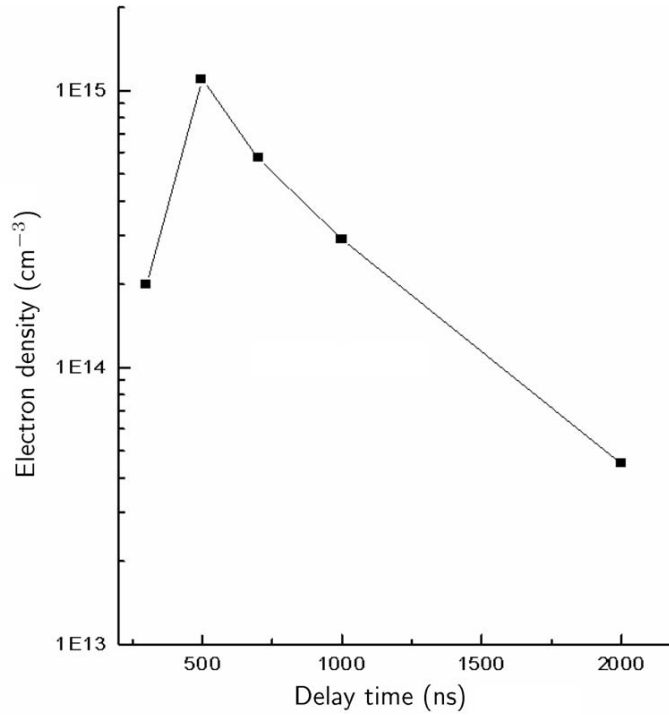


Figure 6. Variation of electron density with delay time.

Table 2. Plasma temperature and electron density as a function of delay time of the detector relative to the onset of the laser pulse on the sample.

Delay time (ns)	Plasma temperature (eV)	Electron density (cm ⁻³)
300	0.78	2.0 × 10 ¹⁴
500	0.84	1.1 × 10 ¹⁵
700	0.79	5.7 × 10 ¹⁴
1000	0.75	2.9 × 10 ¹⁴
2000	0.69	4.5 × 10 ¹³

given in the NIST atomic database. The arithmetic mean of the three values of n_e is represented as the average value of n_e . We have presented these average values as the electron density at several delay times in table 2 and graphically in figure 6. It is observed that after 500 ns delay the electron density decreases exponentially.

The time window where the plasma is optically thin and is also in LTE is inferred from the temporal evolution of the intensity ratio of two Cu I lines, 515.32 and 521.82 nm, which have upper levels having very close energy as shown in table 1. Figure 7 shows the temporal evolution of the intensities of these lines and the intensity ratio between them. We have calculated the intensity ratio for this couple

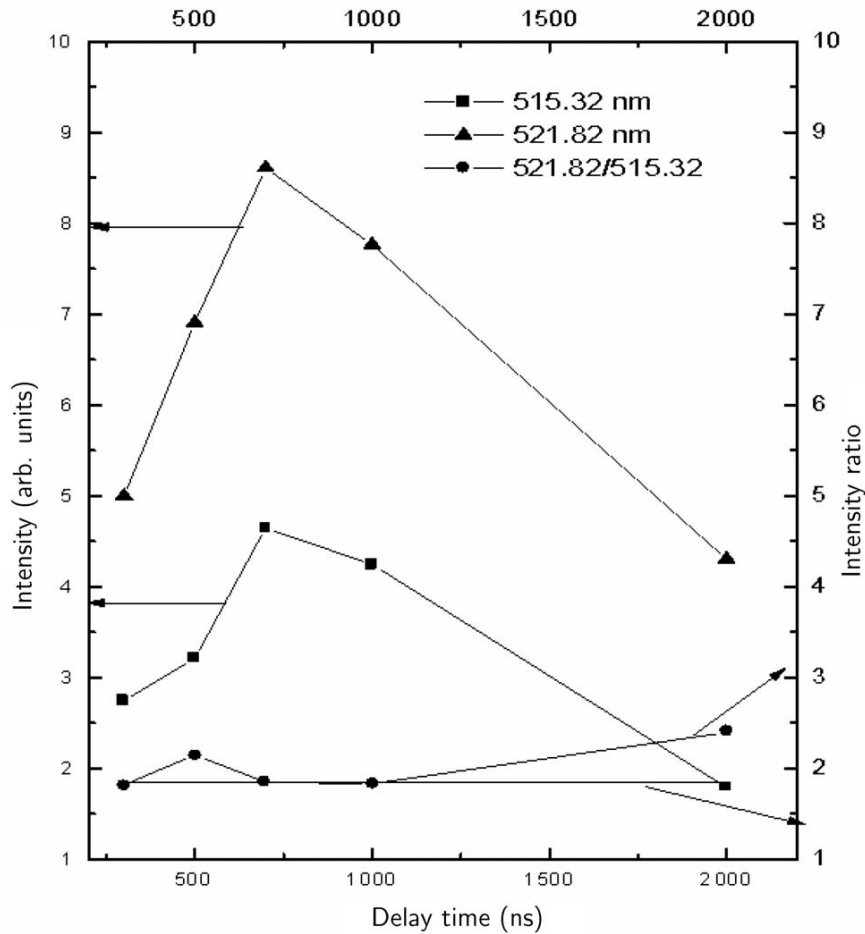


Figure 7. Temporal evolution of intensities of two Cu I lines 515.32 and 521.82 nm and their intensity ratio. The straight line indicates the theoretical intensity ratio = 1.85 for this couple of lines, which is the condition of an optically thin and LTE plasma. The time window for the thin and LTE plasma is 700–1000 ns.

of lines using eq. (6) which is equal to 1.85 and shown this theoretical value as a straight line in the same figure. Comparing the experimental data of the intensity ratio with the theoretical one, we have inferred the time window 700–1000 ns where the LIP produced is thin as well as in LTE.

5. Conclusions

We have determined time-resolved values of the plasma temperature from the Boltzmann plots made from the analysis of five observed Cu I spectral lines. We have also

determined time-resolved values of the electron density from the Saha–Boltzmann equation which relates the electron density with the intensity ratio of atomic and ionic emission lines. The average value of the electron density at a given delay time is calculated by considering the measured intensity ratios of Cu I and Cu II lines at various wavelengths. From the temporal evolution of the intensity ratio of two Cu I lines and matching it with the known value, we have inferred the time window where the plasma is optically thin and is also in LTE. This time window is found to be 700–1000 ns.

Acknowledgement

The authors are thankful to BRNS, DAE, Govt. of India for the financial support provided through a LIBS project (Project No. 2007/34/14-BRNS).

References

- [1] D B Chrisey and G K Hubler, *Pulsed laser deposition of thin films* (Wiley, New York, 1994)
- [2] L J Radziemski and D A Cremers, *Laser-induced plasmas and applications* (Marcel Dekker Inc., New York, 1989)
- [3] A W Miziolek, V Pallesschi and I Schecchter, *Laser-induced breakdown spectroscopy* (Cambridge University Press, Cambridge, 2006)
- [4] D A Cremers and L J Radziemski, *Handbook of laser-induced breakdown spectroscopy* (John Wiley & Sons Ltd, West Sussex, 2006)
- [5] H R Griem, *Principles of plasma spectroscopy* (Cambridge University Press, Cambridge, 1997)
- [6] Y I Lee, S P Sawan, T L Thiem, Y Y Teng and J Sneddon, *Appl. Spectrosc.* **46**, 436 (1992)
- [7] X L Mao, M A Shannon, A J Fernandez and R E Russo, *Appl. Spectrosc.* **49**, 1054 (1995)
- [8] W Pietch, B Dubreuil and A Briand, *Appl. Phys.* **B61**, 267 (1995)
- [9] J D Wu, Q Pan and S C Chen, *Appl. Spectrosc.* **51**, 883 (1997)
- [10] M A Hafez, M A Khedr, F F Elaksher and Y E Gamal, *Plasma Source Sci. Technol.* **12**, 185 (2003)
- [11] J M Gomba, C D' Angelo, D Bertuccelli and G Bertuccelli, *Spectrochimica Acta* **B56**, 695 (2001)
- [12] NIST Atomic Spectra Database, <http://physics.nist.gov>